Available online at www.sciencedirect.com

SciVerse ScienceDirect

Journal of the European Ceramic Society 32 (2012) 465–470

www.elsevier.com/locate/jeurceramsoc

Investigation on the origin of the giant dielectric constant in $CaCu_3Ti_4O_{12}$ ceramics through analyzing $CaCu_3Ti_4O_{12}$–HfO_2 composites

Wen-Xiang Yuan *, S.K. Hark

Department of Physics, The Chinese University of Hong Kong, Shatin, Hong Kong

Received 25 May 2011; received in revised form 15 September 2011; accepted 20 September 2011
Available online 13 October 2011

Abstract

A full range of $CaCu_3Ti_4O_{12}$–HfO_2 (CCTO–HfO_2) composites were prepared by sintering mixtures of the two components at 1000 °C for 10 h. X-ray diffraction studies confirmed the two-phase nature of the composites. The evolution of the microstructure in the composites, in particular, the size distribution of CCTO grains, was examined by scanning electron microscopy. The studies showed that, as more HfO_2 was added, the abnormal grain growth of CCTO and coarsening of the microstructure were gradually suppressed. As a result, the average CCTO grain size was reduced from 50 to 1 μm. The measured dielectric constants agree well with the values calculated from Lichtenecker's logarithmic law, using only the dielectric constants of pure CCTO and HfO_2 as two end points. The agreement suggests to us that the dielectric constant of CCTO is dominated by domain boundaries within the grains rather than by grain boundaries between the grains.

Keywords: A. Sintering; B. Composites; B. Grain size; C. Dielectric properties

1. Introduction

The perovskite-like material calcium copper titanate ($CaCu_3Ti_4O_{12}$, CCTO) is known to process a giant dielectric constant (ε') of about 10^4, which is practically independent of frequencies below 10^6 Hz and insensitive to temperatures over a wide range from 100 to 400 K.[1–4] These remarkable properties endow it with potentially promising applications in the further miniaturization of microelectronics, such as in microwave[5] and dynamic random access memory (DRAM)[6–8] devices. Most studies attribute the cause of the giant dielectric constant of CCTO to extrinsic origins. An "internal barrier layer capacitor" (IBLC) model is often used to explain its strong Maxwell–Wagner like relaxation(s). However, what constitutes the internal barrier remains controversial. Grain boundaries and domain boundaries have been often suggested.[9–16] In CCTO single crystals, grain boundaries are by default absent, leaving the latter as the only possible source. However, their detail structure remains unclear. Twin boundaries, anti-site boundaries and cation-induced planar defects[9] have all been suggested. Polaron effects, possibly associated with stacking faults, have also been suggested.[10,11] For polycrystalline CCTO ceramics, grain boundaries and (or) domain boundaries are the insulating barrier layers responsible for giving rise to a giant dielectric constant. Regardless of the many suggestions of the structure of grain boundaries, an important question remains: which kind of the barrier layers, domain boundaries or grain boundaries, play the dominant role in determining the dielectric properties of CCTO ceramics? On the one hand, scanning probe[12,13] and transmission electron microscopy[14] studies suggest it is the grain boundaries. On the other hand, domain boundaries being dominant has been suggested too.[15–17] We feel that neither suggestion provides a complete picture, as it is possible that the relative importance of domain boundaries to grain boundaries depends on the microstructure. For fine-grain ceramics, the density of grain boundaries is very high, but the grains harbor few, if any, domains. On the other hand, for coarse-grain ceramics, particularly whose processing conditions are prone to result in abnormal grain growth,[3,16–22] the large grains contain many domains. It is instructive to study how the dielectric properties evolve with the change in the relative importance of domain boundaries to grain boundaries. One way to control the grain growth and suppress the abnormal growth of CCTO is to add a second phase, while keeping all of the other

* Corresponding author.
E-mail address: wxyuanster@gmail.com (W.-X. Yuan).

0955-2219/$ – see front matter © 2011 Elsevier Ltd. All rights reserved.
doi:10.1016/j.jeurceramsoc.2011.09.021

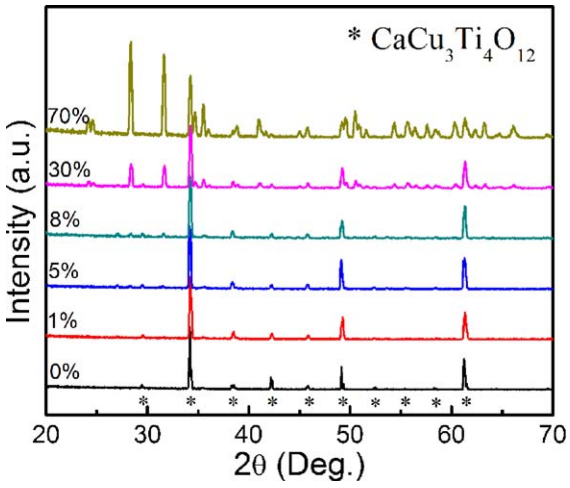

Fig. 1. XRD patterns of CCTO–HfO_2 composites containing different weight percentages of HfO_2.

preparation conditions the same. To this end, the second phase should neither coarsen nor form an alloy with CCTO, and we think hafnia (HfO_2) is a suitable choice. HfO_2, monoclinic in structure below 1700 °C, has a high melting point and is very resistive to impurity diffusion and intermixing at interfaces. More importantly, it is the high-ε' and low leakage gate oxide of the semiconductor industry. Its intrinsic ε' is about 25,[23] with negligible dispersion. Moreover, while the composites[24–28] of perovskites and CCTO have been recently studied, the composites of HfO_2 and CCTO are still to be. Another motivation for adding HfO_2 to CCTO is to help reduce the high dielectric loss of the latter, an important issue in many of its potential applications.

2. Experimental

The CCTO powder was synthesized by a solid state method. Powders of $CaCO_3$, CuO and TiO_2 were mixed, ground for 2 h, and calcined for 10 h at 900 °C to obtain a CCTO powder.[29] Then the resulting powder was ground for another 2 h. After that, different weight percentages (wt%), up to 70%, of a reagent grade HfO_2 powder was added to the CCTO powder and the mixtures were further ground for 20 min. Then the mixtures were cold pressed into 1 cm diameter and 1 mm thick pellets under 4000 psi, and sintered at 1000 °C in air for 10 h (heating rate: 40 °C min^{-1}) to form the composites. Finally, the sintered pellets were polished with SiC papers, and electrodes were applied by painting silver paste on the polished surfaces.

The structures of the composite ceramics were studied by X-ray diffraction (XRD, Rigaku, 40 kV and 160 mA for $2\theta = 20$–$70°$, slit width: 1 mm, step time: 1 s) using the Cu Kα radiation on the as-sintered surfaces of the pellets. Their microstructures were investigated by scanning electron microscopy (SEM, LEO 1450 VP) in the back-scattered secondary electron mode. Dielectric properties were measured at room temperature over frequencies ranging from 40 Hz to 30 MHz by LCR meters (40 Hz–100 kHz, NF 2300; 75 kHz–30 MHz, Agilent 4285).

3. Results and discussion

Existence of two separate phases in the composites was confirmed by XRD. In Fig. 1, we show the XRD patterns of representative samples. The peaks marked by "*" match those of the cubic CCTO phase in the JCPDS file No. 75-2188. The other peaks, which agree with those in the JCPDS file No. 74-1506, are due to the monoclinic HfO_2 phase. For those composites containing less than 5 wt% HfO_2, only peaks of CCTO were observable. As expected, diffraction peaks of CCTO become weaker while those of HfO_2 stronger with increasing HfO_2.

Significant changes in the microstructure of the composites with increasing HfO_2 were revealed by SEM studies, and some of the representative micrographs are shown in Fig. 2. We note that, first of all, among all samples prepared under the same conditions, the largest grains were found in the pure CCTO sample (Fig. 2(a)). With just a small addition of HfO_2, the microstructure changes significantly, as shown in Fig. 2(b). It can be seen that there are two classes of CCTO grains: one is composed of many small grains, and the other of a few large grains. This bimodal size distribution is believed to be a result of abnormal grain growth, which is intimately connected with the presence of a liquid CuO phase during the sintering stage of the sample preparation.[3,24,27] There are far more small grains in the composite containing 1 wt% HfO_2 than in the pure CCTO sample. Moreover, the size of the large grains is also reduced. Although the bimodal distribution of CCTO grains is still apparent, the grain size becomes more homogeneous when more HfO_2 is added. Meanwhile, the presence of the HfO_2 phase is not clearly observed until it reaches to about 5 wt%. The small bright contrasted grains, roughly 1 micrometer in size and embedded within the large CCTO grains shown in Fig. 2(c), were identified as HfO_2 by energy dispersive X-ray analysis (not shown). In the micrograph (Fig. 2(d)) of the composite containing 8 wt% HfO_2, one can see clearly that there are many isolated HfO_2 inclusions within the large CCTO grains. As the amount of HfO_2 increases to more than 20 wt%, HfO_2 grains aggregate and reside between the CCTO grains. At the same time, they suppress the abnormal

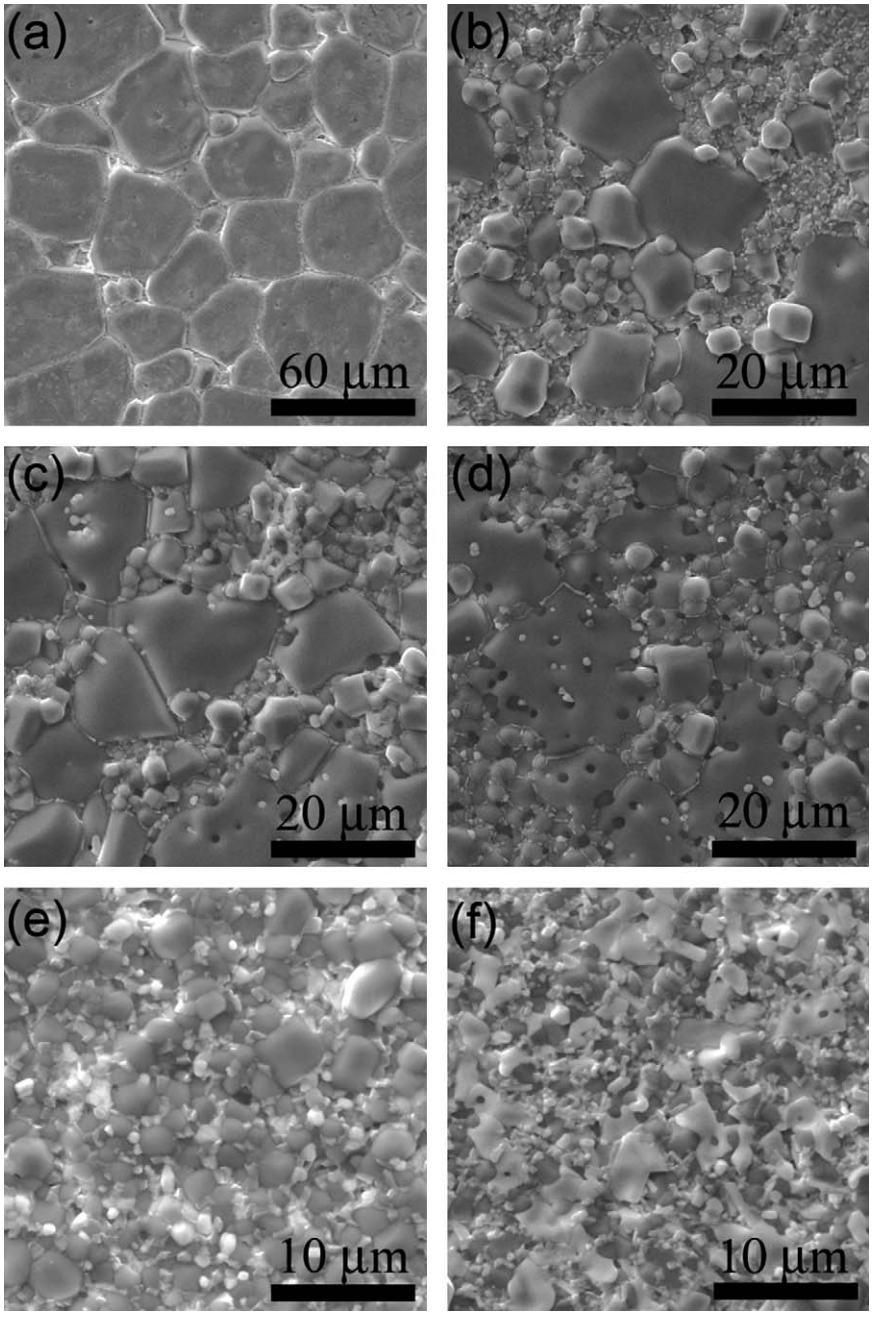

Fig. 2. SEM micrographs of (a) the pure CCTO ceramic and CCTO–HfO_2 composites containing different weight percentages of HfO_2: (b) 1%, (c) 5%, (d) 8%, (e) 30% and (f) 70%.

grain growth, leaving only small CCTO grains in the composites. As an example, the microstructure of the composite containing 30 wt% HfO_2 is shown in Fig. 2(e). In this example, the grain growth of HfO_2 can also be seen. When HfO_2 becomes the major phase of the composite (Fig. 2(f)), not only are there less CCTO grains, there is also a further reduction in size. On the other hand, HfO_2 grains have grown larger. The CCTO grains have already become smaller than the HfO_2 grains. The above observations show that CCTO grain growth is inhibited by adding HfO_2. The abnormal grain growth is completely suppressed when there is only about 20 wt% HfO_2; further increase in HfO_2 results in increasingly smaller CCTO grains.

The evolution of the microstructure with increasing HfO_2 is also reflected in the dielectric constant (ε') and loss ($tan\ \delta$) of the composites. In Fig. 3, the frequency dependence of ε' and $tan\ \delta$ of several selected samples are shown. As shown in Fig. 3(a), consistent with previous reports in the literatures [1–4], there is a plateau over most of the frequency range indicating a wide range of frequency independence in the CCTO–HfO_2 composites, and then a sharp decline in ε' around 1 MHz. Below 1 kHz, $tan\ \delta$ increases with HfO_2; however, it decreases above 1 kHz. ε' of the pure CCTO sample is the highest, and the sample containing 70 wt% HfO_2 (70-wt% HfO_2 sample) has the smallest ε' in all the composite samples. There are two Debye-like relaxations,

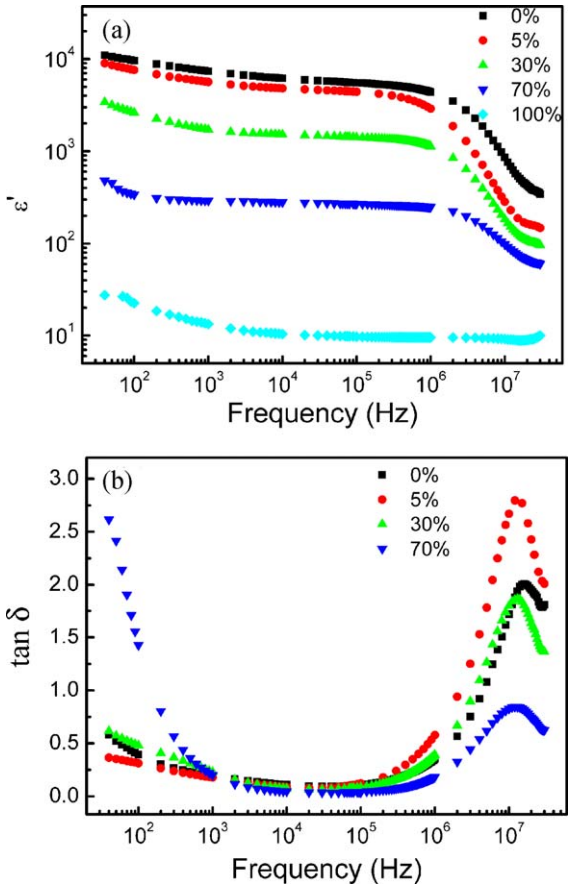

Fig. 3. Frequency-dependent (a) ε' and (b) *tan* δ of CCTO–HfO_2 composites containing different weight percentages of HfO_2.

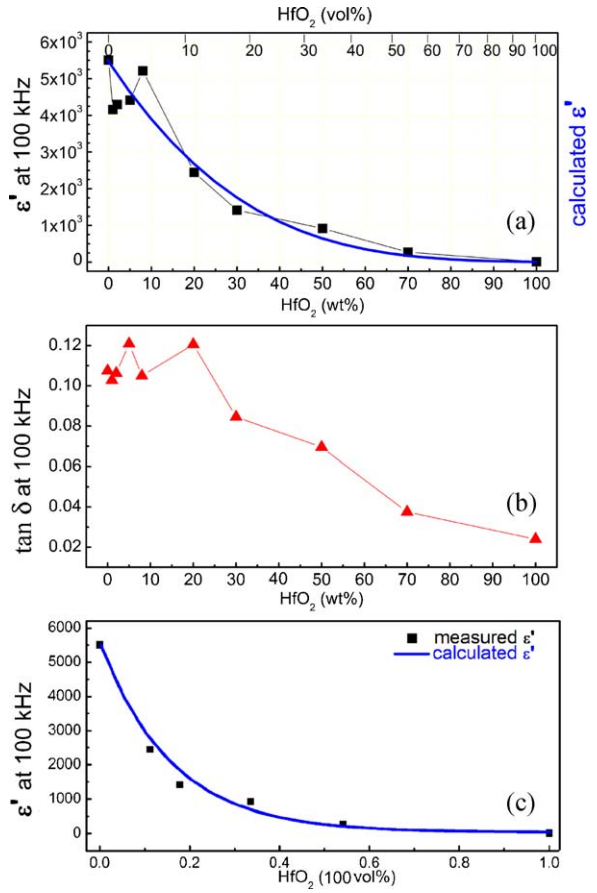

Fig. 4. (a) ε' and (b) *tan* δ of the samples at 100 kHz, (c) ε' of the samples with 0, 20, 30, 50, 70, 100 wt% of HfO_2 at 100 kHz.

one at low and the other at high frequencies, which can also be observed in the dielectric loss plot shown in Fig. 3(b). Large dielectric loss at low frequencies is associated with electrode effects,[30] particularly for the 70-wt% HfO_2 sample. Below the characteristic frequency (~1 MHz), *tan* δ exhibits a relaxation peak, corresponding to the step decrease in ε'. This peak shifts to a lower frequency, from 20 to 10 MHz, after adding HfO_2. This dielectric dispersion, present at high frequencies for all the samples, is less remarkable in the 70-wt% HfO_2 sample, implying that the addition of HfO_2 reduces the dielectric dispersion at high frequencies.

Taking their values at the mid-range frequency (100 kHz) as the representatives of the dielectric properties of the composites, ε' and *tan* δ are listed in Table 1. In order to more clearly show their change with the amounts of HfO_2, we also present the variations of ε' and *tan* δ in Fig. 4(a) and (b), respectively. Also shown in Fig. 4(a) is ε' of the composites calculated from Lichtenecker's logarithmic law[31]: $\ln \varepsilon' = (1-x)\ln \varepsilon'_{CCTO} + x \ln \varepsilon'_{HfO_2}$, where ε'_{CCTO} and ε'_{HfO_2} are the dielectric constants of the pure CCTO and HfO_2 phases, respectively; and x is the volume percentage (vol%) of HfO_2 in the composite. We observe that only a few anomalous points, whose HfO_2 weight ratios are between 1 and 8 wt%, do not fit the Lichtenecker's law well. A basic assumption of Lichtenecker's formula is that the spatial distributions of shapes and orientations of the components in the mixture are statistically random. This assumption is not fulfilled for our composites containing about 1–8 wt% HfO_2, as evidenced by our SEM observations. Within this weight ratio range, the CCTO grains have the abnormal grain growth, resulting in a bimodal size distribution.[32] Furthermore, the much smaller HfO_2 grains tend to occupy preferentially within CCTO grains, resulting in spatially non-random distributions. Thus these measured ε' values do not agree with those calculated. The change of the dielectric loss in the composites with increasing HfO_2 is also anomalous within the same range, as shown in Fig. 4(b).

However, after no less HfO_2 than 20 wt% is added, the abnormal growth of the CCTO grains is suppressed, and HfO_2 aggregates between the CCTO grains. The CCTO grains are gradually covered by HfO_2, constructing a "core–shell" structure in which an insulating HfO_2 barrier layer encloses the semiconducting CCTO grains. In order to exhibit the characteristic of the dielectric properties of the samples with high HfO_2 weight ratios, we plot their dielectric constant in Fig. 4(c). In calculating the effective dielectric constant of the composites, ε' values of the two end points are set equal to the measured values and the volume percentages are converted (Table 1) from the weight percentages using 4.9 g cm^{-3} for the density of CCTO[33] and 9.68 g cm^{-3} for HfO_2.[34] Considering the fact that no adjustable parameters were used, the calculated ε' values agree very well with the measured ones. We have verified that

Table 1
Microstructural parameters and dielectric properties of $CaCu_3Ti_4O_{12}$-HfO_2 composites.

HfO_2 (wt%)	HfO_2 (vol%)	Density (g cm^{-3})[a]	CCTO grain size (μm)	HfO_2 grain size (μm)	ε' at 100 kHz	$tan\,\delta$ at 100 kHz
0	0	4.9	50	Nil	5510.05	0.0932
1	0.51	4.92	6.3	Nil	4157.92	0.0638
2	1.02	4.95	6.5	Nil	4297.74	0.0635
5	2.60	5.02	6.8	1	4413.55	0.0792
8	4.22	5.10	8	1	5217.34	0.0787
20	11.23	5.44	3	1	2446.36	0.1069
30	17.83	5.75	2.8	1	1415.87	0.0632
50	33.61	6.51	1.6	2	918.35	0.0584
70	54.15	7.49	1	2.3	269.34	0.0348
100	100	9.68	Nil	Nil	9.68	0.0224

[a] Density is calculated using the densities of CCTO[33] (4.9 g cm^{-3}) and HfO_2 [34] (9.68 g cm^{-3}).

similarly good agreements between the calculated and measured ε' values of the composites also occur at other frequencies. Lichtenecker's law has been known to be applicable to composites, and its nature has recently been shown to be more fundamental than previously thought.[35] Since the dielectric constant of HfO_2 is intrinsic and maintains the same value, the agreement suggests that the dielectric constant of the CCTO phase has to be the same, too. However, the grain boundary effect does not explain the same ε' value. Based on it, the dielectric constant of CCTO is proportional to the CCTO grain size on the condition that the grain-boundary thickness and dielectric constant of the bulk (or grain) are relatively unchanged with the grain size. For example, the SEM studies in Fig. 2 have shown that the CCTO grains decrease in size from 50 μm for the pure CCTO to 1 μm for the 70-wt% HfO_2 sample, consequently yielding a smaller dielectric constant for the CCTO in the 70-wt% HfO_2 sample. However, based on the above argument, the dielectric constant of CCTO should be unchanged with the decrease in the CCTO grain size. Therefore, it suggests that the grain boundary effect does not play the dominant role in controlling the dielectric constant of CCTO. A more probable explanation is that the domain boundary effect determines ε' of CCTO, which implies domain boundaries have to exist even in micron-sized CCTO grains. The data shown here give an indirect evidence of the existence of the domain boundaries, which we think are the origin of the giant dielectric constant of CCTO.[15–17] This assumption unifies the origin of the dielectric constant of CCTO as the domain boundary effect, in both poly-crystals (ceramics) and single crystals. In brief, when more HfO_2 ($\geq$20 wt%) is added, the dielectric constant agrees well with the Lichtenecker's law (Fig. 4(c)), and the dielectric loss is reduced (Fig. 4(b)).

4. Conclusions

In summary, we have prepared and studied a full range of CCTO–HfO_2 composites. With increasing HfO_2, the commonly occurred abnormal grain growth of the CCTO phase and the associated bimodal grain distribution are gradually suppressed. The presence of HfO_2 also reduces the CCTO grain size from 50 to 1 μm. Despite these changes, the dielectric constant of the CCTO phase remains the same, as inferred from the agreement between the measured dielectric constants of the composites and those calculated by Lichtenecker's law, except in cases where the grain distributions are far from random. These results suggest that it is the domain boundaries rather than the grain boundaries that contribute to the giant dielectric constant of polycrystalline CCTO ceramics.

Acknowledgement

This work was partially supported by grants from the Research Grants Council of the Hong Kong Special Administrative Region, China (Project No. 411807).

References

1. Ramirez AP, Subramanian MA, Gardel M, Blumberg G, Li D, Vogt T, et al. Giant dielectric constant response in a copper–titanate. *Solid State Commun* 2000;**115**:217–20.
2. Subramanian MA, Sleight AW. $ACu_3Ti_4O_{12}$ and $ACu_3Ru_4O_{12}$ perovskites: high dielectric constants and valence degeneracy. *Solid State Sci* 2002;**4**:347–51.
3. Fang TT, Shiau HK. Mechanism for developing the boundary barrier layers of $CaCu_3Ti_4O_{12}$. *J Am Ceram Soc* 2004;**87**:2072–9.
4. Thomas P, Sathapathy LN, Dwarakanath K, Varma KB. Microwave synthesis and sintering characteristics of $CaCu_3Ti_4O_{12}$. *Bull Mater Sci* 2007;**30**:567–70.
5. Subramanian MA, Dong L, Duan N, Reisner BA, Sleight AW. High dielectric constant in $ACu_3Ti_4O_{12}$ and $ACu_3Ti_3FeO_{12}$ phase. *J Solid State Chem* 2000;**151**:323–5.
6. Ezhilvalavan S, Tseng TY. Process in the developments of (Ba,Sr)TiO_3 (BST) thin films for giga-bit era DRAMs. *Mater Chem Phys* 2000;**65**:227–48.
7. Kretly LC, Almeida AFL, Olivera RSD, Sasaki JM, Soombra ASB. Electrical and optical properties of $CaCu_3Ti_4O_{12}$ (CCTO) substrates for microwave devices and antennas. *Microwave Opt Technol Lett* 2003;**39**:145–50.
8. Almeida AFL, Fechine PBA, Goes JC, Miranda MA, Miranda MAR, Sombra ASB. Dielectric properties of $BaTiO_3$(BTO)–$CaCu_3Ti_4O_{12}$(CCTO) composite screen-printed thick films for high dielectric constant devices in the medium frequency (MF) range. *Mater Sci Eng B* 2004;**111**:113–23.
9. Wang C, Zhang HJ, He PM, Cao GH. Ti-rich and Cu-poor grain-boundary layers of $CaCu_3Ti_4O_{12}$ detected by X-ray photoelectron spectroscopy. *Appl Phys Lett* 2007;**91**:052910.
10. Zhang L, Tang ZJ. Polaron relaxation and variable-range-hopping conductivity in the giant-dielectric-constant material $CaCu_3Ti_4O_{12}$. *Phys Rev B* 2004;**70**:174306.
11. Bueno PR, Tararan R, Parra R, Joanni E, Ramirez MA, Ribeiro WC, et al. A polaronic stacking fault defect model for $CaCu_3Ti_4O_{12}$ material: an

approach for the origin of the huge dielectric constant and semiconducting coexistent features. *J Phys D: Appl Phys* 2009;**42**:055404.
12. Chung SY, Kim ID, Kang SJL. Strong nonlinear current–voltage behaviour in perovskite-derivative calcium copper–titanate. *Nat Mater* 2004;**3**: 774–8.
13. Kalinin SV, Shin J, Veith GM, Baddorf AP, Lobanov MV, Runge H, et al. Real space imaging of the microscopic origins of the ultrahigh dielectric constant in polycrystalline $CaCu_3Ti_4O_{12}$. *Appl Phys Lett* 2005;**86**, 102902.
14. Wu L, Zhu Y, Park S, Shapiro S, Shirane G, Tafto J. Defect structure of the high-dielectric-constant perovskite $CaCu_3Ti_4O_{12}$. *Phys Rev B* 2005;**71**:014118.
15. Bueno PR, Ramírez MA, Varela JA, Longo E. Dielectric spectroscopy analysis of $CaCu_3Ti_4O_{12}$ polycrystalline systems. *Appl Phys Lett* 2006;**89**:191117.
16. Fang TT, Liu CP. Evidence of the internal domains for inducing the anomalously high dielectric constant of $CaCu_3Ti_4O_{12}$. *Chem Mater* 2005;**17**:5167–71.
17. Ramírez MA, Bueno PR, Tararam R, Cavalheiro AA, Longo E, Varela JA. Evaluation of the effect of the stoichiometric ratio of Ca/Cu on the electrical and microstructural properties of the $CaCu_3Ti_4O_{12}$ polycrystalline system. *J Phys D: Appl Phys* 2009;**42**:185503 [8 pp.].
18. Shao SF, Zhang JL, Zheng P, Zhong WL, Wang CL. Microstructure and electric properties of $CaCu_3Ti_4O_{12}$ ceramics. *J Appl Phys* 2006;**99**, 084106.
19. Kim KM, Lee JH, Lee KM, Kim DY, Riu DH, Lee SB. Microstructural evolution and dielectric properties of Cu-deficient and Cu-excess $CaCu_3Ti_4O_{12}$ ceramics. *Mater Res Bull* 2008;**43**:284–91.
20. Lebey T, Guillemet S, Bley V, Boulos M, Durand B. Origin of the colossal permittivity and possible application of CCT ceramics. In: *IEEE 2005 Electro Comp Tech Confer, vol. 2*. 2005. p. 1248–53.
21. Ramírez MA, Bueno PR, Varela JA, Longo E. Nonohmic and dielectric properties of $Ca_2Cu_2Ti_4O_{12}$ polycrystalline system. *Appl Phys Lett* 2006;**89**:212102.
22. Ramírez MA, Bueno PR, Longo E, Varela JA. Conventional and microwave sintering of $CaCu_3Ti_4O_{12}/CaTiO_3$ ceramic composites: nonohmic and dielectrical properties. *J Phys D: Appl Phys* 2008;**41**:152004 [5 pp.].
23. Zhao XY, Vanderbilt D. First-principles study of structural, vibrational, and lattice dielectric properties of hafnium oxide. *Phys Rev B* 2002;**65**, 233106.
24. Fang TT, Chung HY, Liou SC. Manifestation of the electrode-contact effect on the dielectric response and impedance spectra of $CaSiO_3$-doped $CaCu_3Ti_4O_{12}$. *J Appl Phys* 2009;**106**, 054106.
25. Ramirez MA, Parra R, Reboredo MM, Varela JA, Castro MS, Ramajo L. Elastic modulus and hardness of $CaTiO_3$, $CaCu_3Ti_4O_{12}$ and $CaTiO_3/CaCu_3Ti_4O_{12}$ mixture. *Mater Lett* 2010;**64**:1226–8.
26. Bueno PR, Ribeiro WC, Ramirez MA, Varela JA, Longo E. Separation of dielectric and space charge polarizations in $CaCu_3Ti_4O_{12}/CaTiO_3$ composite polycrystalline systems. *Appl Phys Lett* 2007;**90**:142912.
27. Fang TT, Lin WJ, Lin CY. Evidence of the ultrahigh dielectric constant of $CaSiO_3$-doped $CaCu_3Ti_4O_{12}$ from its dielectric response, impedance spectroscopy, and microstructure. *Phys Rev B* 2007;**76**:045115.
28. Yu HT, Liu HX, Hao H, Luo DB, Cao MH. Dielectric properties of $CaCu_3Ti_4O_{12}$ ceramics modified by $SrTiO_3$. *Mater Lett* 2008;**62**: 1353–5.
29. Yuan WX, Hark SK, Mei WN. Effective synthesis to fabricate a giant dielectric-constant material $CaCu_3Ti_4O_{12}$ via solid state reactions. *J Ceram Process Res* 2009;**10**:696–9.
30. Yuan WX, Hark SK, Mei WN. Investigation of triple extrinsic origins of colossal dielectric constant in $CaCu_3Ti_4O_{12}$ ceramics. *J Electrochem Soc* 2010;**157**:G117–20.
31. Lichtenecker K. Dielectric constant of natural and synthetic mixtures. *Phys Z* 1926;**27**:115–58.
32. Pan MJ, Bender BA. A bimodal grain size model for predicting the dielectric constant of calcium copper titanate ceramics. *J Am Ceram Soc* 2005;**88**:2611–4.
33. Grimshaw RW. *The chemistry and physics of clays and allied ceramic materials*. London: Ernest Benn Limited; 1971.
34. Marshall PA, Potter RJ, Jones AC, Chalker PR, Taylor S, Critchlow GW, et al. Growth of hafnium aluminate thin films by liquid injection MOCVD using alkoxide precursors. *Chem Vap Depos* 2004;**10**:275–9.
35. Simpkin R. Derivation of Lichtenecker's logarithmic mixture formula from Maxwell's equations. *IEEE Trans Microwave Theory Tech* 2010;**58**:545–50.